INTERNATIONAL JOURNAL FOR NUMERICAL METHODS IN FLUIDS
Int. J. Numer. Meth. Fluids **26**: 987–1000 (1998)

MULTIDIMENSIONAL UPWIND SCHEMES FOR THE SHALLOW WATER EQUATIONS

H. PAILLÈRE[1], G. DEGREZ* AND H. DECONINCK

von Karman Institute for Fluid Dynamics, Chaussée de Waterloo 72, B-1640 Rhode St-Genèse, Belgium

SUMMARY

A multidimensional discretisation of the shallow water equations governing unsteady free-surface flow is proposed. The method, based on a residual distribution discretisation, relies on a characteristic eigenvector decomposition of each cell residual, and the use of appropriate distribution schemes. For uncoupled equations, multidimensional convection schemes on compact stencils are used, while for coupled equations, either system distribution schemes such as the Lax–Wendroff scheme or scalar schemes may be used. For steady subcritical flows, the equations can be partially diagonalised into a purely convective equation of hyperbolic nature, and a set of coupled equations of elliptic nature. The multidimensional discretisation, which is second-order-accurate at steady state, is shown to be superior to the standard Lax–Wendroff discretisation. For steady supercritical flows, the equations can be fully diagonalised into a set of convective equations corresponding to the steady state characteristics. Discontinuities such as hydraulic jumps, are captured in a sharp and non-oscillatory way. For unsteady flows, the characteristic equations remain coupled. An appropriate treatment of the coupling terms allows the discretisation of these equations at the scalar level. Although presently only first-order-accurate in space and time, the classical dam-break problem demonstrates the validity of the approach. © 1998 John Wiley & Sons, Ltd.

KEY WORDS: shallow water equations; multidimensional upwinding

1. INTRODUCTION

The shallow water equations (SWE) describe the motion of unsteady free-surface flows subjected to gravity forces, such as atmospheric and oceanographic flows, mountain torrents, coastal rivers and estuary flows, tsunamis and flows resulting from the collapse of hydraulic dams. The SWE are the hydraulic analogue of the Euler equations of gas dynamics [1]. In particular, they admit discontinuous solutions, called hydraulic jumps, which are the analogue of shock waves, with a correspondence between the water elevation h (SWE) and the gas density ρ (Euler equations).

As a result of the analogy between the equations of gas dynamics and the SWE, it is tempting to apply the same successful methods developed for gas dynamics problems to hydraulic problems governed by the SWE. The MacCormack scheme in particular seems to have been very popular among hydraulic engineers. Recently, several applications of the flux difference splitting scheme of Roe to the SWE have been proposed [2–5]. Finite element

* Correspondence to: von Karman Institute for Fluid Dynamics, Chaussée de Waterloo 72, B-1640 Rhode St-Genèse, Belgium.
[1] Present address: CEA/DMT/SEMT, Laboratoire de Transferts Thermiques et Mécanique des Fluides, 91191 Gif-sur-Yvette Cedex, France.

CCC 0271–2091/98/080987–14$17.50

Received September 1995
Revised January 1997

schemes based on the Taylor–Galerkin method (the finite element version of the 'Lax–Wendroff' scheme) have also been developed [6,7]. Genuinely multidimensional upwind discretisation based on 'simple wave models' have been reported in References [8,9], with promising reports for supercritical flows. However, wave models which use gradient-dependent directions often suffer from convergence problems. Furthermore, as for the Euler equations, wave model-based methods are ill-suited for subcritical flows [10]. Indeed, recasting the three equations of the shallow water system into a set of five or six convective equations corresponding to the different waves, and discretising each one of them using a scalar upwind scheme, leads to excessive dissipation. The key property that a multidimensional residual decomposition should possess is the so-called 'linearity preserving' (LP) property which guarantees second-order-accuracy at steady state (but presently only first-order-accuracy for unsteady flows). The models described in Reference [8] do not satisfy this property and it is one of the objectives of this paper to improve on this aspect.

The method proposed in this paper is based on a multidimensional characteristic-based 'diagonalisation' of the equations which, by construction, satisfies the LP property. The method, which uses the flow angle and where defined, the Froude angles (analogous to the Mach angles in compressible flow) as upwinding directions, is an extension of the 'hyperbolic/elliptic' splitting described in Reference [11] for the Euler equations. Steady subcritical and supercritical flows are simulated using this approach. For the subcritical example, a comparison is made with a standard Lax–Wendroff residual distribution scheme, showing the benefit of the multidimensional discretisation. For the supercritical example, a hydraulic jump is simulated and captured in a sharp and non-oscillatory way. Although finite volume total variation diminishing (TVD) methods perform just as well on such a test case, it must be realised that the methods described here use compact finite element type stencils and do not explicitly make use of limiter functions to guarantee positivity. Furthermore, the multidimensional schemes are robust and can handle severely distorted meshes with very little loss of accuracy [12]. LP models can also be developed for unsteady flows, for which the equations remain coupled. A characteristic-based model is proposed and applied to the classical dam-break problem, in which the flow resulting from the partial collapse of a hydraulic dam is simulated. Although presently only first-order-accurate in space and time, the method compares well with standard finite volume schemes.

2. THE SHALLOW WATER EQUATIONS

The SWE in conservative form are given by:

$$\frac{\partial U}{\partial t}+\frac{\partial F}{\partial x}+\frac{\partial G}{\partial y}=S, \tag{1}$$

where U is the vector of conservative variables, and F and G are the fluxes,

$$U=\begin{pmatrix} h \\ hu \\ hv \end{pmatrix}, \qquad F=\begin{pmatrix} hu \\ hu^2+g\dfrac{h^2}{2} \\ huv \end{pmatrix}, \qquad G=\begin{pmatrix} hv \\ huv \\ hv^2+g\dfrac{h^2}{2} \end{pmatrix}. \tag{2}$$

h is the depth of water, u and v are the depth-averaged velocity components, and g is the acceleration due to gravity, $g=9.81\ \mathrm{m\ s^{-2}}$. S is a source term, accounting for friction losses and bed slopes. In the present study, only the homogeneous case is considered ($S=0$). In quasi-linear form, the equations take the following form:

$$\frac{\partial U}{\partial t} + A\frac{\partial U}{\partial x} + B\frac{\partial U}{\partial y} = 0, \tag{3}$$

with the Jacobian matrices $A = \partial F/\partial U$ and $B = \partial G/\partial U$:

$$A = \begin{bmatrix} 0 & 1 & 0 \\ -a^2 - u^2 & 2u & 0 \\ -uv & v & u \end{bmatrix}, \qquad B = \begin{bmatrix} 0 & 0 & 1 \\ -uv & v & u \\ a^2 - v^2 & 0 & 2v \end{bmatrix}, \tag{4}$$

where $a = \sqrt{gh}$ represents the shallow water wave speed. The ratio $Fr = V/a$, where $V = \sqrt{u^2 + v^2}$, is a non-dimensional number called the Froude number, which is the analogue of the Mach number in compressible gas dynamics. Like the Euler equations, the SWE form a hyperbolic system, so that the Jacobian matrix $C = A\cos\theta + B\sin\theta$ has real eigenvalues and eigenvectors for all values of θ. These are given by:

$$\lambda^1 = u\cos\theta + v\sin\theta, \qquad \lambda^2 = u\cos\theta + v\sin\theta + a, \qquad \lambda^3 = u\cos\theta + v\sin\theta - a, \tag{5}$$

$$L = \begin{bmatrix} l_1 \\ l_2 \\ l_3 \end{bmatrix} = \frac{1}{a}\begin{bmatrix} u\sin\theta - v\cos\theta & -\sin\theta & \cos\theta \\ \frac{1}{2}(a - u\cos\theta - v\sin\theta) & \frac{1}{2}\cos\theta & \frac{1}{2}\sin\theta \\ \frac{1}{2}(a + u\cos\theta + v\sin\theta) & \frac{1}{2}\cos\theta & \frac{1}{2}\sin\theta \end{bmatrix}, \tag{6}$$

$$R = L^{-1} = [r_1 r_2 r_3] = \begin{bmatrix} 0 & 1 & 1 \\ -a\sin\theta & u + a\cos\theta & u - a\sin\theta \\ a\cos\theta & v + a\sin\theta & v - a\sin\theta \end{bmatrix}. \tag{7}$$

3. ONE-DIMENSIONAL CASE

In one dimension ($\theta = 0$), the flux difference splitting scheme of Roe [2–5] can be recast as a fluctuation splitting scheme. Assuming forward Euler time stepping, it takes the form:

$$U_i^{n+1} = U_i^n - \frac{\Delta t}{\Delta x_i}\left[(x_i - x_{i-1})\sum_{\ell=1}^{3}\beta_i^{[x_{i-1},x_i],\ell}\lambda^\ell(l_\ell\nabla U)r_\ell + (x_{i+1} - x_i)\sum_{\ell=1}^{3}\beta_i^{[x_i,x_{i+1}],\ell}\lambda^\ell(l_\ell\nabla U)r_\ell\right], \tag{8}$$

with $\beta_i^{[x_{i-1},x_i],\ell} = \max(0, \lambda^\ell)/\lambda^\ell$ and $\beta_i^{[x_i,x_{i+1}],\ell} = \min(0, \lambda^\ell)/\lambda^\ell$ are scalar distribution coefficients, defined for each wave. For conservation, the eigenvalues and eigenvectors in cell $[x_{i-1}, x_i]$ are evaluated at the Roe-average state [2]:

$$\hat{h} = \frac{h_{i-1} + h_i}{2}, \qquad \hat{u} = \frac{\sqrt{h_{i-1}}u_{i-1} + \sqrt{h_i}u_i}{\sqrt{h_{i-1}} + \sqrt{h_i}}, \qquad \hat{a} = \sqrt{g\hat{h}}, \tag{9}$$

and similarly for the average state in cell $[x_i, x_{i+1}]$. Note that these expressions are *not* the same as those derived for the Euler equations, and do not generalise to 2D. This is better understood by examining how the average state $\hat{U}$ is derived. Explicitly writing out the conditions for the Roe-linearisation (known as property U):

$$\Delta F = A(\hat{U})\Delta U, \tag{10}$$

$$\hat{U}(U, U) = U, \tag{11}$$

where $\Delta(\cdot) = (\cdot)_R - (\cdot)_L$, this becomes:

$$u_R h_R - u_L h_L = 1 \times (u_R h_R - u_L h_L), \tag{12}$$

$$u_R^2 h_R - u_L^2 h_L + \frac{g}{2}(h_R^2 - h_L^2) = (g\hat{h} - \hat{u}^2)(h_R - h_L) + 2\hat{u}(u_R h_R - u_L h_L). \tag{13}$$

Separating the gravity terms from the convective terms, this becomes:

$$\frac{g}{2}(h_R^2 - h_L^2) = g\hat{h}(h_R - h_L), \tag{14}$$

$$\hat{u}^2(h_R - h_L) - 2\hat{u}(u_R h_R - u_L h_L) + u_R^2 h_R - u_L^2 h_L = 0. \tag{15}$$

The equation in $\hat{h}$ yields the solution $\hat{h} = (h_R + h_L)/2$. The quadratic equation in $\hat{u}$ has two roots, only one of which reduces to u when $u_R = u_L = u$ and $h_R = h_L$:

$$\hat{u} = \frac{\sqrt{h_R}u_R + \sqrt{h_L}u_L}{\sqrt{h_R} + \sqrt{h_L}}. \tag{16}$$

4. TWO-DIMENSIONAL CASE

To extend the fluctuation-splitting formulation to the 2D SWE, a conservative linearisation must be sought, such that for every triangular cell:

$$\Phi^T = \oint_{\partial T} F\,\mathrm{d}y - G\,\mathrm{d}x = S_T[A(\hat{U})U_x + B(\hat{U})U_y], \quad \forall T, \tag{17}$$

where S_T is the area of cell T. It is obvious that the trick of separating the gravity terms from the convective terms no longer works. Instead, a global solution $(\hat{h}, \hat{u}, \hat{v})$ of this system must be defined. Assuming the left-hand-side (LHS) is known (it can be evaluated by the trapezium rule of integration), the following system must be solved:

$$\mathrm{LHS}_1 = (g\hat{h} - \hat{u}^2)h_x + 2\hat{u}(hu)_x - \hat{u}\hat{v}h_y + \hat{v}(hu)_y + \hat{u}(hv)_y, \tag{18}$$

$$\mathrm{LHS}_2 = -\hat{u}\hat{v}h_x + \hat{v}(hu)_x + \hat{u}(hv)_x + (g\hat{h} - \hat{v}^2)h_y + 2\hat{v}(hv)_y. \tag{19}$$

If $\hat{h}$ is the arithmetic average over the cell, $\hat{h} = (h_i + h_j + h_k)/3$ (i, j and k denote the vertices of the cell), a non-linear system of two equations in two unknowns $(\hat{u}, \hat{v})$ remains, which may be solved using a Newton-type procedure. This linearisation is similar to the linearisation of Abgrall [13], derived for the Euler equations. Although conceptually straightforward, convergence problems were encountered when solving this system, especially in regions of uniform flow. Thus, results presented in this work were obtained using a non-conservative linearisation, basically the formal extension of the 1D linearisation,

$$\hat{h} = \frac{h_i + h_j + h_k}{3}, \qquad \hat{u} = \frac{\sqrt{h_i}u_i + \sqrt{h_j}u_j + \sqrt{h_k}u_k}{\sqrt{h_i} + \sqrt{h_j} + \sqrt{h_k}}, \qquad \hat{a} = \sqrt{g\hat{h}}. \tag{20}$$

$$\hat{v} = \frac{\sqrt{h_i}v_i + \sqrt{h_j}v_j + \sqrt{h_k}v_k}{\sqrt{h_i} + \sqrt{h_j} + \sqrt{h_k}}$$

In Reference [9], source terms were added to correct for the difference between the exact contour integral and the quasi-linear form evaluated at the parameter average state. In the present work, no such correction was added, as it did not prove detrimental to either accuracy or convergence (see Section 5.1).

4.1. Multidimensional upwind schemes for scalar convection

The second step of the extension of the method to two dimensions concerns the development of upwind distribution schemes for the scalar convection equation,

$$\frac{\partial W}{\partial t} + \vec{\lambda} \cdot \nabla W = 0. \tag{21}$$

The residual or 'fluctuation' ϕ^T is obtained by integrating this equation over a triangular cell T:

$$\phi^T = \iint_T \vec{\lambda} \cdot \nabla \mathrm{W} \, \mathrm{d}\Omega. \tag{22}$$

In the residual distribution approach, fractions of ϕ^T are distributed to the vertices of the cell, with scalar coefficients β_i^T, summing up to one for consistency. After assembling contributions from all the cells, each nodal value can be updated as:

$$W_i^{n+1} = W_i^n - \frac{\Delta t}{S_i} \sum_T \beta_i^T \phi^T, \tag{23}$$

where S_i represents the area of the median dual cell around node i, and the forward Euler explicit time marching scheme was used. Both linear and non-linear upwind distribution schemes on unstructured triangular meshes, have been developed over the past years [14], with built-in properties such as positivity and linearity preservation (second-order-accuracy at steady state). A new interpretation of the PSI scheme is given here, which is a non-linear, positive and linearity preserving fluctuation splitting scheme. This interpretation is derived from Sidilkover and Roe's formulation for non-linear finite volume and fluctuation splitting schemes [15]. Assuming constant convection speed $\vec{\lambda}$ and linear variations of W over a triangular cell, the residual ϕ^T may be expressed as:

$$\phi^T = S_T \vec{\lambda} \cdot \nabla W = \sum_{i=1}^{3} k_i W_i^n, \tag{24}$$

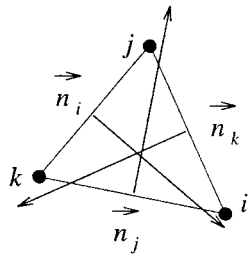

Figure 1. Triangle and inward normals $\vec{n}_i$.

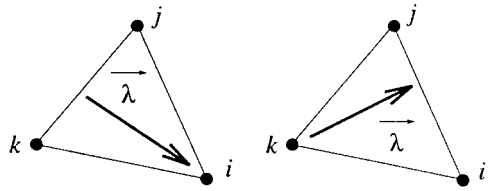

Figure 2. One-target case (left) and two-target case (right).

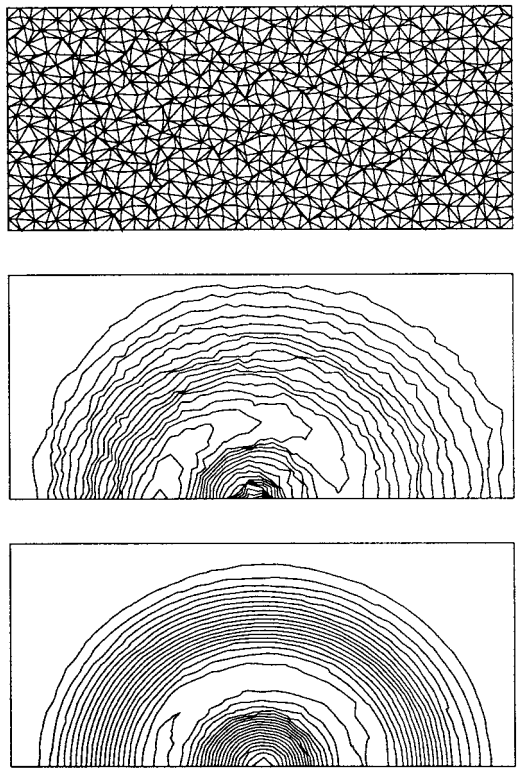

Figure 3. Rotational convection problem: distorted mesh (top) and solution isolines of the first-order upwind FV scheme (middle) and PSI scheme (bottom).

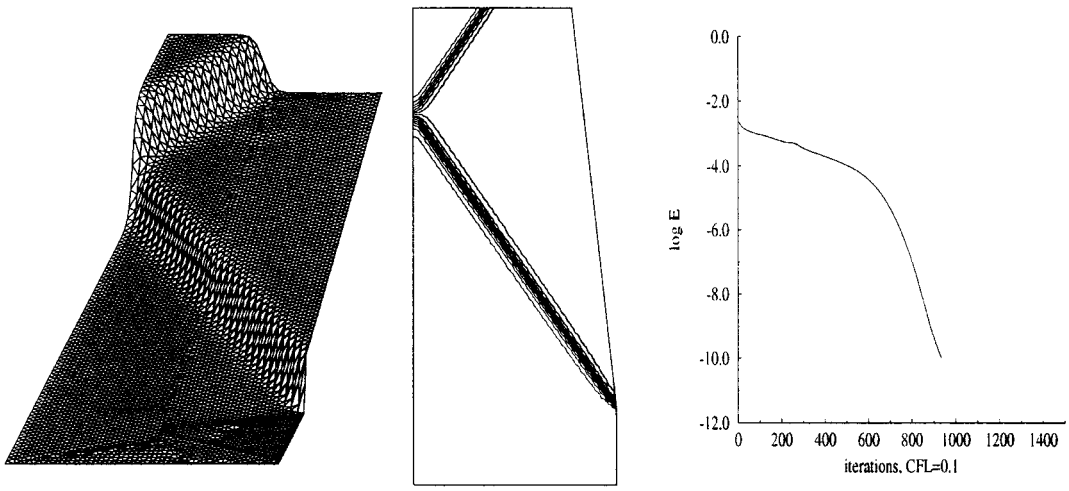

Figure 4. Supercritical mountain torrent: water elevation, Froude number and convergence history ($E = \|\mathrm{Res}_{i,1}\|_{L_\infty}$), obtained with the hyperbolic/elliptic splitting and the PSI scheme.

where S_T is the area of the cell, and k_i is called the inflow parameter, and is defined as $k_i = 1/2\ \vec{\lambda}\cdot\vec{n}_i$, $\vec{n}_i$ being the inward normal opposite node i and scaled by the length of the edge (Figure 1). $\Sigma_{i=1}^{3}\vec{n}_i = \vec{0}$, therefore, $\Sigma_{i=1}^{3} k_i = 0$. $k_i > 0$ signifies that i is a downstream node (or target node) of the triangle, and should therefore receive a contribution. In the two-target situation sketched in Figure 2, where i and j denote the two downstream modes, a linear positive scheme, called the N scheme, is given by:

$$\beta_i^N \phi^T = k_i(W_i^n - W_k^n), \qquad \beta_j^N \phi_T = k_j(W_j^n - W_k^n). \tag{25}$$

This scheme is not linearity preserving, since $\phi^T = 0 \nRightarrow \beta_i^N \phi^T = 0$, $\beta_j^N \phi^T = 0$. This is equivalent to the statement that the distribution coefficients of the N scheme are unbounded. On the other hand, an LP scheme can be obtained by limiting the distribution coefficients, i.e. by applying a limiter function $\Psi(r)$ to the unbounded coefficients β_i^N:

$$\beta_i^{\lim} = \Psi(\beta_i^N), \quad \text{where } \beta_i^N = \frac{k_i(W_i^n - W_k^n)}{\phi^T}. \tag{26}$$

Of course, the distribution coefficients to the two downstream nodes must add up to one for consistency. This implies that $\Psi(r) + \Psi(1-r) = 1$, a property satisfied by the minmod limiter, $\Psi(r) = \max(0, \min(1, r))$. It can be easily verified that the resulting scheme is identical to the PSI scheme proposed in [14]. In Figure 3, a comparison between the PSI scheme and the first-order upwind finite volume scheme (on the dual mesh) is shown. The comparison is significant because both schemes share the same compact stencil, and require the same computational effort. However, the PSI scheme combines both positivity and linearity preservation, and produces much more accurate solutions, even on severely distorted meshes.

4.2. *'Hyperbolic/elliptic' splitting model*

The motivation for developing multidimensional upwind schemes for hyperbolic systems of equations, is to incorporate into the scheme the mechanisms by which information travels. For steady supercritical flow, the SWE behave much like the Euler equations, in the sense that the equations take on a purely convective character (they can be completely diagonalised), and disturbances propagate within a cone of dependence, defined by the Froude angles:

$$\tan\theta = \frac{\pm 1}{\sqrt{Fr^2 - 1}}. \tag{27}$$

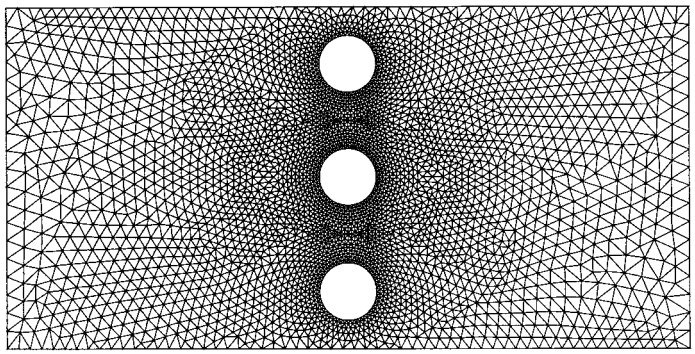

Figure 5. Subcritical flow past a row of circular bridge pillars: unstructured mesh.

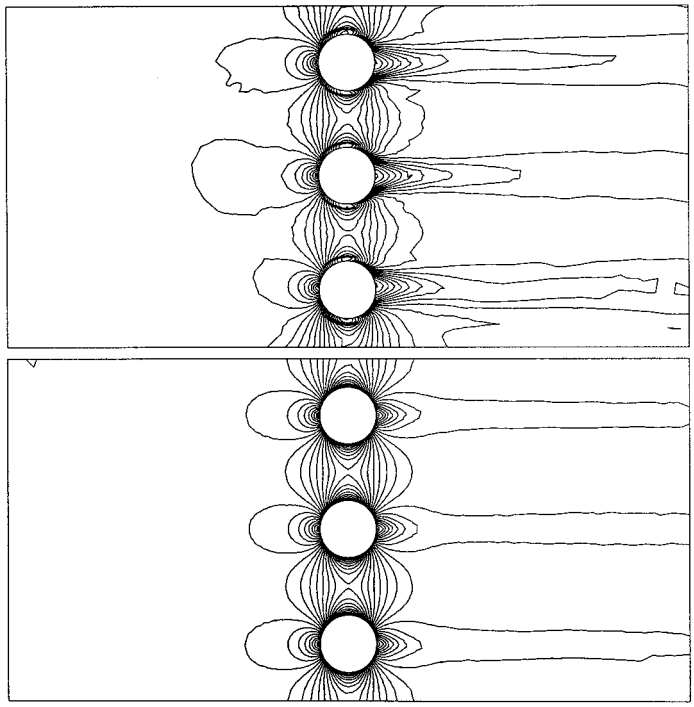

Figure 6. Subcritical flow past a row of circular bridge pillars: Froude number isolines ($\Delta Fr = 0.01$) obtained with the Lax–Wendroff scheme on the full system (top, $Fr_{\min} = 0.0013$ and $Fr_{\max} = 0.2685$) and with the hyperbolic/elliptic splitting (bottom, $Fr_{\min} = 0.0001$ and $Fr_{\max} = 0.2534$).

Indeed, rewriting the steady SWE in the streamwise co-ordinate system (ξ, η), with some manipulation they become:

$$\frac{\partial H_0}{\partial \xi} = 0, \tag{28}$$

$$\frac{\partial C^+}{\partial \xi} + \frac{1}{\sqrt{Fr^2 - 1}} \frac{\partial C^+}{\partial \eta} = 0, \tag{29}$$

$$\frac{\partial C^-}{\partial \xi} - \frac{1}{\sqrt{Fr^2 - 1}} \frac{\partial C^-}{\partial \eta} = 0, \tag{30}$$

where $\partial H_0 = 1/h\,(a^2 - \tilde{u}^2)\,\partial h + 1/h\,\tilde{u}\,\partial \tilde{u}h$, and $\partial C^{+,-} = \pm (a^2 - \tilde{u}^2)/\sqrt{Fr^2 - 1}\,\partial h + Fr\,\partial \tilde{v}$ ($\tilde{u}$ and $\tilde{v}$ are the components of $\vec{u}$ in the (ξ, η) co-ordinate system). The quantity ∂H_0, is actually the exact differential expression of the total energy $H_0 = gh + V^2/2$, consisting of the potential energy gh and the kinetic energy $V^2/2$. At steady state, similar to entropy and total enthalpy in the case of the Euler equations, H_0 is conserved along streamlines. The gravity wave variables C^+ and C^-, remain constant along the Froude lines. For subcritical flows, these are no longer defined, and the equations in the variables $(\partial h, \partial \tilde{v})$ become coupled, taking on a purely elliptic character. In summary, a splitting can be derived, similar in principle to the 'hyperbolic/elliptic' splitting derived for the Euler equations [11], incorporating the following features:

- convection of total energy H_0 along streamlines and discretisation of this equation using an upwind convection operator (PSI scheme);
- in supercritical flow, convection of characteristics C^+ and C^- along the Froude lines and discretisation of these equations using an upwind convection operator (PSI scheme);
- in subcritical flow, coupling of the gravity wave equations and discretisation using a system distribution scheme such as the Lax–Wendroff scheme. For a system written in quasi-linear form (3), the Lax–Wendroff distribution matrices $\mathscr{B}_i^T$ take the following form [16]:

$$\mathscr{B}_i^T = \frac{1}{3} I + \frac{\Delta t}{4 S_T} (A, B) \cdot \vec{n}_i, \tag{31}$$

corresponding to the update scheme:

$$U_i^{n+1} = U_i^n - \frac{\Delta t}{S_i} \sum_T \mathscr{B}_i^T \Phi^T. \tag{32}$$

4.3. Characteristic decomposition model

A multidimensional decomposition model, inspired by the characteristic decomposition method of Deconinck, Hirsch and Peuteman [17] and the 'pseudo Mach angle' approach described in Reference [10], is obtained by defining a vector of characteristic variables $\partial W = L^* \partial U$ depending on two parameters (θ, ψ):

$$L^* = \frac{1}{a} \begin{bmatrix} u \sin\psi - v \cos\psi & -\sin\psi & \cos\psi \\ \frac{1}{2}(a - u\cos\theta - v\sin\theta) & \frac{1}{2}\cos\theta & \frac{1}{2}\sin\theta \\ \frac{1}{2}(a + u\cos\theta + v\sin\theta) & -\frac{1}{2}\cos\theta & -\frac{1}{2}\sin\theta \end{bmatrix}, \tag{33}$$

$$R^* = \varpi \begin{bmatrix} 0 & \varpi & \varpi \\ -a\sin\theta & u\varpi + a\cos\psi & u\varpi - a\cos\psi \\ a\cos\theta & v\varpi + a\sin\psi & v\varpi - a\sin\psi \end{bmatrix}, \tag{34}$$

where $\varpi = \cos\theta\cos\psi + \sin\theta\sin\psi$. Substituting this into the system of SWE, an approximate diagonalisation is obtained, leading to the expression of the flux divergence:

$$F_x + G_y = \sum_{\ell=1}^{3} [\vec{\lambda}^\ell \cdot \nabla W + q^\ell] r^\ell, \tag{35}$$

where $\vec{\lambda}^\ell$ are the characteristic ray speed vectors, given by:

$$\vec{\lambda}^1 = u\vec{1}_x + v\vec{1}_y, \tag{36}$$

$$\vec{\lambda}^2 = \left(u + \frac{a}{2}(\cos\theta + \cos\psi/\varpi)\vec{1}_x\right) + \left(v + \frac{a}{2}(\sin\theta + \sin\psi/\varpi)\vec{1}_y\right), \tag{37}$$

$$\vec{\lambda}^3 = \left(u - \frac{a}{2}(\cos\theta + \cos\psi/\varpi)\vec{1}_x\right) + \left(v - \frac{a}{2}(\sin\theta + \sin\psi/\varpi)\vec{1}_y\right). \tag{38}$$

$\vec{1}_x$ and $\vec{1}_y$ are the unit vectors in the x- and y-directions, respectively. The q^ℓ are coupling terms, corresponding to the off-diagonal terms of the matrices L^*AR^* and L^*BR^*. In supercritical flows, the angle θ is taken to be equal to the Froude angle ($\sin\theta = 1/Fr$), and in subcritical flow, it is taken to be equal to a 'pseudo Froude angle' ($\tan\theta = 1/\sqrt{1 - Fr^2}$). To maximise the determinant of the transformation, ψ is taken to be equal to θ ($\varpi = 1$). Each scalar equation is then discretised using an upwind convection scheme, such as the PSI scheme.

4.4. Boundary conditions

The flow tangency condition at the wall is imposed through a strong characteristic formulation. The nodal residual at a boundary point is first obtained by looping over the interior cells. Then, a correction is added in the form of a gravity wave, whose intensity is such that the condition $\Delta\vec{u}\cdot\vec{n}=0$ is satisfied.

At a subcritical inlet, two conditions must be imposed. In this case, it was decided to impose the total energy $H_0=gh+V^2/2$, as well as the flow angle α. The flow velocity $V=\sqrt{u^2+v^2}$ is extrapolated from the interior domain.

At a subcritical outlet, one physical condition must be applied. The water elevation h was chosen for this work, and the other variables, namely hu and hv are extrapolated from the interior.

4.5. Time integration schemes

In this work, a multistage Runge–Kutta scheme was implemented, consisting of four stages:

$$\begin{aligned} &U^{(0)}=U_i^n,\\ &U^{(p)}=U^{(0)}-\alpha^{(p)}\frac{\Delta t}{S_i}\,\mathrm{Res}_i(U^{(p-1)}),\quad p=1,2,3,4,\\ &U_i^{n+1}=U^{(4)}. \end{aligned} \tag{39}$$

For steady state calculations, the time step Δt was defined locally so as to satisfy the local stability condition. For unsteady flow computations, a constant time step Δt was used, based on the stability condition determined from the initial conditions:

$$\Delta t\le\frac{\min_T\sqrt{S_T}}{\sqrt{g}\,\max_i h_i}. \tag{40}$$

It should be pointed out that the LP residual distribution schemes described in Section 4.1 are only second-order-accurate in space at *steady state*, while their space accuracy reduces to first-order for unsteady problems (see e.g. Reference [18]). This deficiency can, however, be remedied by the use of a consistent mass matrix formulation, as shown in a recent study by Deconinck and Degrez [19], but requires an implicit solver.

5. NUMERICAL RESULTS

5.1. Oblique hydraulic jump

The supercritical flow ($Fr=2.5$) in a 5° contracting channel is simulated. As explained previously ('hyperbolic/elliptic' splitting), the SWE diagonalise completely in this case, and the use of positive, high-order shock-capturing scalar convection schemes such as the PSI scheme, leads to monotone and accurate solutions. Figure 4 shows a carpet plot of the water elevation h and the isolines of the Froude number computed by this diagonalisation approach, as well as the convergence history of the L_∞ norm of the first component of the nodal residual Res_i, as defined in Equation (39), i.e. of the nodal residual of the continuity equation. Note that the nodal residual is the discretisation of the divergence of fluxes (minus the source term when present) and is therefore independent of the time step, as well as of the time stepping

algorithm. The numerical value of the water height downstream of the reflected shock is found to be 1.5270, which is very close to the exact value of 1.5273 found by the Rankine–Hugoniot jump relations. Thus, the conservation error made in the linearisation process remains very small, as also remarked in Reference [9].

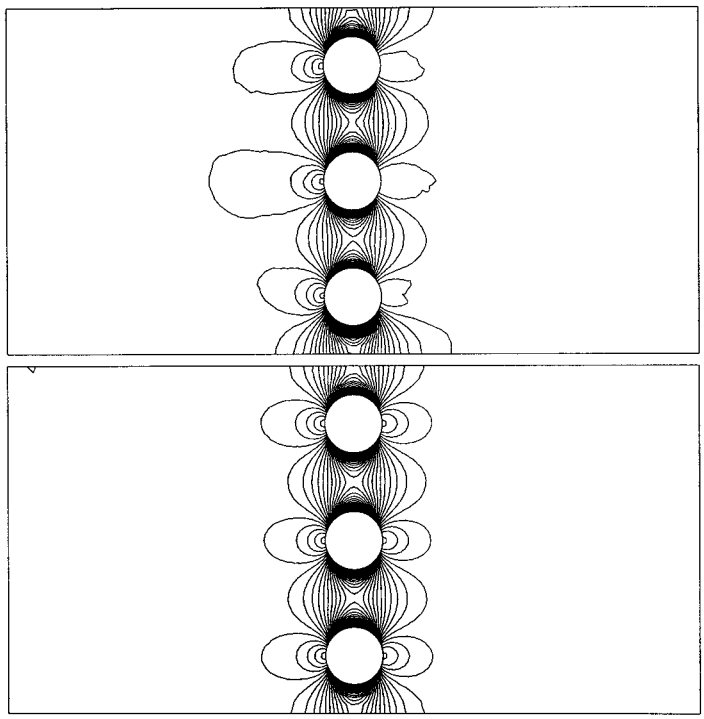

Figure 7. Subcritical flow past a row of circular bridge pillars: water elevation contours ($\Delta h = 10^{-3}$ m) obtained with the Lax–Wendroff scheme on the full system (top, $h_{\min} = 0.9662$ m and $h_{\max} = 1.0049$ m) and with the hyperbolic/elliptic splitting (bottom, $h_{\min} = 0\ 9662$ m and $h_{\max} = 1.0049$ m).

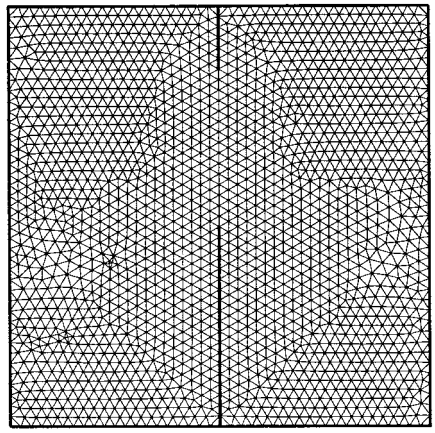

Figure 8. Geometry of dam-break problem and unstructured mesh, consisting of 1906 vertices and 3600 cells.

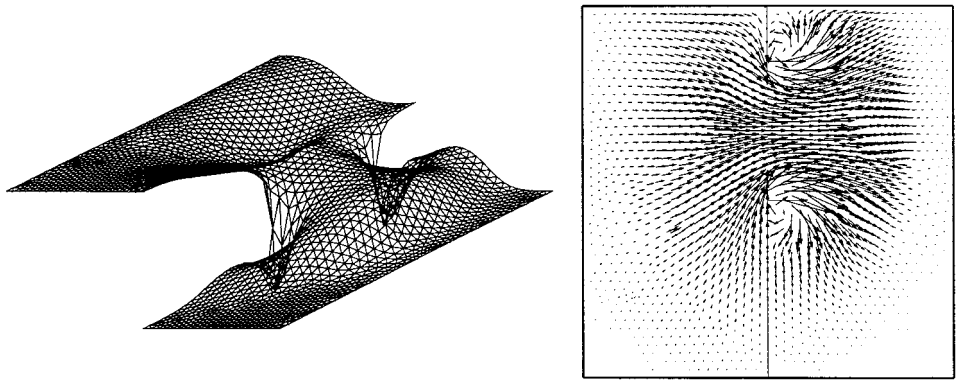

Figure 9. Carpet plot of water elevation and velocity vectors at time $t = 7.2$ s.

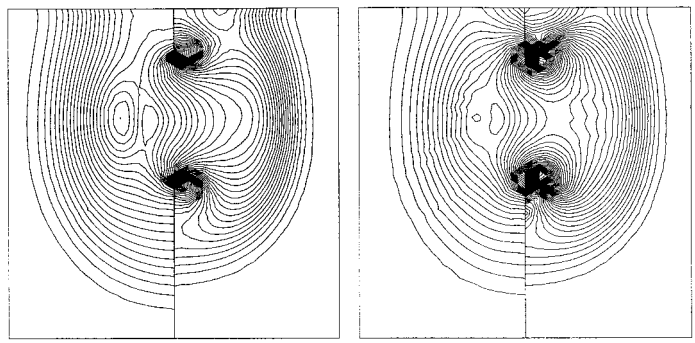

Figure 10. Isolines of water elevation (left, $h_{\min} = 4.05$ m, $h_{\max} = 10.0$ m and $\Delta h = 0.1$ m) and Froude number (right, $Fr_{\min} = 0.0$, $Fr_{\max} = 1.01$ and $\Delta Fr = 0.02$), at time $t = 7.2$ s.

5.2. Subcritical flow past a row of circular bridge pillars

The steady subcritical flow ($Fr = 0.1$) past a row of circular bridge pillars is computed. The mesh which consists of 3500 vertices is shown in Figure 5.

Figures 6 and 7 show Froude number and water elevation contours for two different decomposition models/distribution schemes, namely the Lax–Wendroff distribution scheme on the full system of equations on one hand, and the hyperbolic/elliptic splitting model with PSI discretisation of the uncoupled convection equation for H_0 and Lax–Wendroff discretisation of the 2×2 coupled gravity wave system on the other hand. As observed previously for the Euler equations [11,12], the latter model is seen to be much less dissipative, as indicated by the much more symmetric character of the solution. It should be stressed that this reduced dissipation is due to the uncoupling of the convection equation for H_0 rather than the use of the PSI distribution scheme on the latter equation. In fact, using a linear LP scheme such as the LDA scheme or the scalar Lax–Wendroff scheme on this equation would further reduce dissipation, at the expense of the loss of the positivity property which ensures the absence of spurious oscillations of H_0.

5.3. Two-dimensional dam-break problem

To demonstrate the applicability of the residual distribution schemes to unsteady problems, keeping in mind the accuracy limitation of the formulation as discussed in Section 4.5, the

sudden break of a hydraulic dam is now simulated. This test case has been computed in several recent papers [2,3,5], and allows the comparison of the multidimensional method with upwind, dimensionally split solvers, for a similar number of grid points. The geometry of the problem is illustrated in Figure 8: at time $t = 0$, a 75 m long breach in the wall of the dam is created, releasing a vast quantity of water (tailwater/reservoir height ratio is 0.5) which spreads in all directions. The purpose of the simulation is to predict the two-dimensional propagation of the bore.

The carpet plot and isolines of the solution at $t = 7.2$ s are plotted in Figure 9 Figure 10. Despite the first-order space accuracy of the present formulation, the solution agrees well with previous studies [3,5], whereas the solution of Glaister [2] does not predict the water accumulation on the right wall in the same manner.

6. CONCLUSIONS

In this study, a multidimensional discretisation of the SWE was proposed, based on characteristic decomposition methods and upwind convection schemes. A conservative linearisation was proposed, but not implemented. This aspect requires further investigation. It was noted that the 1D Roe linearisation does not extend naturally to 2D, unlike for the Euler equations. Numerical results were shown, illustrating the 'hydraulic jump' capturing capability of the scheme, as well as its ability to compute subcritical flows. Finally, a time-dependent problem, namely the partial collapse of a hydraulic dam, was simulated. The results obtained with the present method are in good qualitative agreement with published results obtained using dimensionally-split schemes.

REFERENCES

1. P.A. Thomson, *Compressible Fluid Dynamics*, McGraw-Hill, New York, 1972.
2. P. Glaister, 'Flux difference splitting for open-channel flows', *Int. j. numer. methods fluids*, **16**, 629–654 (1993).
3. D. Ambrosi, 'Approximation of shallow water equations by Roe's Riemann solver', *Int. j. numer. methods fluids*, **20**, 157–168 (1995).
4. H. Zhang and M. Reggio, 'A finite volume solver for the shallow water equations in varying bed environments', *Comp. Fluid Dyn.*, **3**, 233–2507 (1994).
5. F. Alcrudo and P. Garcia-Navarro, 'A high-resolution Godunov-type scheme in finite volumes for the 2D shallow water equations', *Int. j. numer. methods fluids*, **16**, 489–505 (1993).
6. F.E. Hicks and P.M. Steffler, 'Comparison of finite element methods for the St. Venant equations', *Int. j. numer. methods fluids*, **20**, 99–113 (1994).
7. O.C. Zienkiewicz and P. Ortiz, 'A split-characteristic based finite element model for the shallow water equations', *Int. j. numer. methods fluids*, **20**, 1061–1080 (1995).
8. P. Garcia-Navarro, M.E. Hubbard and A. Priestley, 'Genuinely multidimensional upwinding for the 2D shallow water equations' *J. Comp. Phys.*, **121**, 79–93 (1995).
9. M.E. Hubbard, P. Garcia-Navarro and M.J. Baines, 'Conservative multidimensional upwinding for the shallow water equations', Technical report, Department of Mathematics, *Numerical Analysis Report 4/95*, University of Reading, 1995.
10. H. Paillère, J.-C. Carette and H. Deconinck, 'Multidimensional upwind and SUPG methods for the solution of the compressible flow equations on unstructured grids', in VKI LS 1994-05, *Comput. Fluid Dyn., 1994.*
11. H. Paillère, H. Deconinck and P.L. Roe, 'Conservative upwind residual-distribution schemes based on the steady characteristics of the Euler equations', *12th AIAA CFD Conference*, *Paper 95-1700*, San Diego, 1995.
12. H. Paillère, Multidimensional upwind residual distribution, schemes for the Euler and Navier–Stokes equations on unstructured grids', *Ph.D. Thesis*, Université Libre de Bruxelles, 1995.
13. R. Abgrall, 'Approximation of the multidimensional Riemann problem in compressible fluid mechanics by a Roe type method', *SIAM J. Numer. Anal.*, 1994. Submitted for publication.
14. R. Struijs, H. Deconinck and P.L. Roe, 'Fluctuation splitting schemes for the 2D Euler equations', in VKI LS 1991-01, *Comput. Fluid Dyn.*, 1991.

15. D. Sidilkover and P.L. Roe, 'Unification of some advection schemes in two dimensions', *Technical Report 95-10*, ICASE, 1995.
16. K.W. Morton, P.N. Childs and M.A. Rudgyard, 'The cell vertex method for steady compressible flow', in *Proc. IMA Conf*., *Numerical Methods for Fluid Dynamics*, *111*, Oxford University Press, London, 1988, pp. 137–152.
17. H. Deconinck, Ch. Hirsch and J. Peuteman, 'Characteristic decomposition methods for the multidimensional Euler equations', in *Lecture Notes in Physics*, Vol. 264, Springer, Berlin, 1986.
18. R. Struijs, 'Numerical methods for advection-diffusion problems', in C.B. Vreugdenhil and B. Koren, (eds). *Notes on Numerical Fluid Mechanics*, Vieweg, Wiesbaden, Vol. 45, pp. 261–289, 1993.
19. H. Deconinck and G. Degrez, 'Monotone shock capturing cell vertex schemes for the Euler and Navier–Stokes equations. *15th Int. Conf. on Numerical Methods in Fluid Dynamics*, Monterey, June 24–25, 1996.

